

Parameterized Temperature Scaling for Boosting the Expressive Power in Post-Hoc Uncertainty Calibration

Christian Tomani,¹ Daniel Cremers,¹ Florian Buettner²

¹Technical University of Munich, ²Siemens AG

christian.tomani@tum.de, cremers@tum.de, buettner.florian@siemens.com

Abstract

We address the problem of uncertainty calibration and introduce a novel calibration method, Parametrized Temperature Scaling (PTS). Standard deep neural networks typically yield uncalibrated predictions, which can be transformed into calibrated confidence scores using post-hoc calibration methods. In this contribution, we demonstrate that the performance of accuracy-preserving state-of-the-art post-hoc calibrators is limited by their intrinsic expressive power. We generalize temperature scaling by computing prediction-specific temperatures, parameterized by a neural network. We show with extensive experiments that our novel accuracy-preserving approach consistently outperforms existing algorithms across a large number of model architectures, datasets and metrics.

1 Introduction

1.1 Post-hoc uncertainty calibration

Due to their high predictive power, neural network based systems are increasingly used for decision making in real world applications. Models deployed in such real-world settings, require not only high accuracy, but also reliability and uncertainty-awareness. Especially in safety critical applications such as autonomous driving or in automated factories where average case performance is insufficient, a reliable estimate for the predictive uncertainty of models is crucial. This can be achieved via well-calibrated calibrated confidence scores that are representative of the true likelihood of a prediction.

Since standard neural networks tend to yield systematically overconfident predictions [5], a number of algorithms for post-hoc calibration have been proposed.

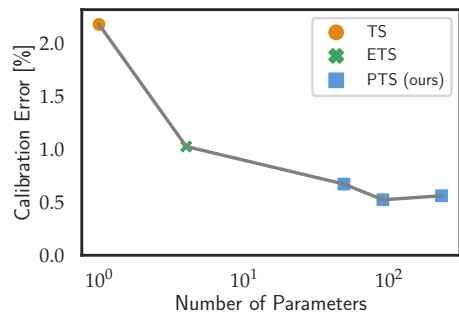


Figure 1: With increased expressive power, temperature scaling-based models yield lower expected calibration errors (ECE). Increasing model capacity from one parameter (TS) to 4 parameters (ETS) results in a 53% reduction in calibration error. Increasing model capacity further (our approach) yields an additional reduction of 49% in calibration error. All post-hoc calibration models were optimized to calibrate a Resnet152 trained on ImageNet.

These algorithms include parametric approaches that transform the outputs of neural networks based on simple linear models in form of Platt-scaling or Temperature scaling. Alternative non-parametric approaches include histogram- or regression-based models such as histogram-binning or isotonic regression. Recent research efforts have shown that combining and extending these base techniques [24, 10] results in a plethora of approaches where no single approach performs best across datasets and model architectures. In addition, all accuracy-preserving state-of-the-art approaches are collectively limited by a low expressive power (or model capacity): Temperature scaling [5] fits a single scalar parameter, extended temperature scaling [24] is based on a weighted ensemble of 3 fixed temperatures. While non-parametric models are more expressive, they usually do not preserve model accuracy and the accuracy of trained models may decrease substantially after calibration [5, 24]. Importantly, all previously proposed

accuracy-preserving approaches are based on a fixed calibration map, that transforms all uncalibrated predictions of a neural network into calibrated predictions in the same manner without leveraging information from individual predictions.

We hypothesize that the performance of accuracy-preserving post-hoc calibration models is intrinsically limited by their expressive power, which stems from a lack of modeling a prediction-specific transformation.

1.2 Contributions

In this work we make the following contributions:

- We show that the limiting factor of TS-based post-hoc calibrators is the expressive power of the underlying calibration model.
- We generalize temperature scaling based on a highly expressive neural network that computes *prediction-specific* temperatures; we refer to our accuracy-preserving post-hoc calibration approach as Parameterized Temperature Scaling (PTS)
- We show that our approach has a similar data-efficiency as standard prediction-agnostic post-hoc calibrators
- We demonstrate in exhaustive experiments that PTS outperforms existing methods across a wide range of datasets, models and evaluation metrics.

2 Related Work

In this section, we review existing approaches for post-hoc calibration of trained neural networks. For this type of post-processing method a validation set, drawn from the generative distribution of the training data, is used to rescale the outputs returned by a trained neural network such that in-domain predictions are well calibrated. Related work can be categorized along two distinct axes, namely parametric vs non-parametric methods and accuracy-preserving methods vs. those where accuracy can change after calibration. While non-parametric approaches tend to have a higher expressive power than parametric models, most non-parametric methods suffer from the drawback that they do not preserve the accuracy of trained neural networks.

2.1 Non-parametric methods

A popular non-parametric post-processing approach is histogram binning [22]. In brief, all uncalibrated confidence scores \hat{P}_i are partitioned into M bins with borders typically chosen such that either all bins contain the same number of samples or are of the same size. Next,

a calibrated score Q_m is assigned to each bin by optimizing a bin-wise squared loss on the validation set. For each new prediction, the uncalibrated confidence score \hat{P}_{pr} is then replaced by the calibrated score associated to the bin \hat{P}_{pr} falls into. Extensions to histogram binning include isotonic regression [23] and Bayesian Binning into Quantiles (BBQ) [14]. For isotonic regression, uncalibrated confidence scores are divided into M intervals and a piecewise constant function f is fitted on the validation set. This isotonic function is then used to transform uncalibrated outputs to calibrated scores. BBQ is a Bayesian generalization of histogram binning using the concept of Bayesian model averaging. A recently proposed alternative to histogram-based methods is Gaussian Process based calibration [21]. While most non-parametric methods do not preserve the accuracy of trained neural networks, [24] have recently introduced an accuracy-preserving extension of isotonic regression by imposing strict isotonicity on the isotonic function.

2.2 Parametric methods

In addition to these non-parametric approaches, also parametric alternatives for post-processing confidence scores exist. For example, the idea of Platt scaling [16] is based on transforming the non-probabilistic outputs (logits) $z_i \in \mathbb{R}$ of a binary classifier to calibrated confidence scores. While initially proposed in the context of support vector machines, Platt scaling has also been used for calibrating other classifiers, including neural networks. More specifically, the logits are transformed to calibrated confidence scores \hat{Q}_i using logistic regression $\hat{Q}_i = \sigma(az_i + b)$, where σ is the sigmoid function. The two parameters a and b are fitted by optimising the negative log-likelihood of the validation set.

[5] generalized Platt scaling to the multi-class case: Temperature Scaling (TS) is a simple but popular post-processing approach where a scalar parameter T is used to re-scale the logits of a trained neural network. In the case of C -class classification, the logits are a C -dimensional vector $\mathbf{z}_i \in \mathbb{R}^C$, which are typically transformed into confidence scores \hat{P}_i using the softmax function σ_{SM} . For temperature scaling, logits are rescaled with temperature T and transformed into calibrated confidence scores \hat{Q}_i using σ_{SM} as

$$\hat{Q}_i = \max_c \sigma_{SM}(\mathbf{z}_i/T)^{(c)} \quad (1)$$

T is learned by minimizing the negative log likelihood of the validation set. [24] have recently introduced an extended temperature scaling, where calibrated predictions are obtained by a weighted sum of predictions re-scaled via three individual temperature terms: an adjustable temperature (as in vanilla temperature scaling), a fixed temperature of 1 and a fixed temperature of ∞ . In contrast to the non-parametric methods introduced

Table 1: Expected calibration error ECE¹. For all architectures our approach outperformed baseline post-hoc calibrators

	Base	IROvA	IROvA-TS	IRM	PBMC	TS	ETS	PTS
CIFAR_LeNet5	1.91	1.99	1.93	1.57	2.14	1.92	1.67	1.4
CIFAR_VGG19	7.92	1.1	0.77	1.03	1.67	1.38	1.34	0.6
CIFAR100_LeNet5	7.55	1.71	2.53	3.52	2.69	1.72	1.28	1
CIFAR100_VGG19	12.96	5.73	2.89	5.31	3.05	3.64	2.12	0.85
Imagenet_ResNet50	6.26	6.6	5.66	2.86	3.47	1.85	1.35	0.97
Imagenet_ResNet152	6.39	6.56	5.47	2.88	3.49	2.18	1.03	0.52
Imagenet_VGG19	2.1	6.06	5.9	1.79	3.2	2.22	1.34	0.99
Imagenet_DenseNet169	6.14	6.62	5.64	2.74	3.4	1.97	1.08	0.71
Imagenet_EfficientNetB7	2.99	6.2	6.13	3.05	1.52	5.91	2.94	1.48
Imagenet_Xception	13.25	8.32	5.44	5.34	3.27	4.4	1.84	1.06
Imagenet_MobileNetV2	5.19	4.49	5.49	1.69	2.06	3.49	1.79	1.01

above or other parametric multi-class calibrators such as vector scaling/matrix scaling [5] or Dirichlet based scaling [13], Temperature Scaling-based methods have the advantage that they do not change the accuracy of the trained neural network. Since re-scaling does not affect the ranking of the logits, also the maximum of the softmax function remains unchanged. In this work, we build on temperature scaling in order to leverage its accuracy-preserving nature and introduce a generalized formulation that overcomes its limited expressive power.

2.3 Other related work

Orthogonal approaches have been proposed based on intrinsically uncertainty-aware networks such as Bayesian neural networks, where typically a prior distribution over the weights is specified and, given the training data, a posterior distribution over the weights is inferred [7, 4, 9, 20, 15, 2]. Other, non-Bayesian approaches to uncertainty-aware neural networks include for example Deep Ensembles [11]. However, in contrast to post-hoc calibration methods these intrinsically uncertainty-aware neural networks are very costly to train.

3 Definitions and problem set-up

Let $X \in \mathbb{R}^D$ and $Y \in \{1, \dots, C\}$ be random variables that denote the D -dimensional input and labels in a classification task with C classes with a ground truth joint distribution $\pi(X, Y) = \pi(Y|X)\pi(X)$. The dataset \mathcal{D} consists of N i.i.d. samples $D = \{(X_n, Y_n)\}_{n=1}^N$ drawn from $\pi(X, Y)$. Let $h(X) = (\hat{Y}, \hat{Z})$ be the output of a trained neural network classifier h predicting a class \hat{Y} and an associated unnormalized logit tuple \hat{Z} based on X . \hat{Z} is then transformed into a confidence score \hat{P} associated to

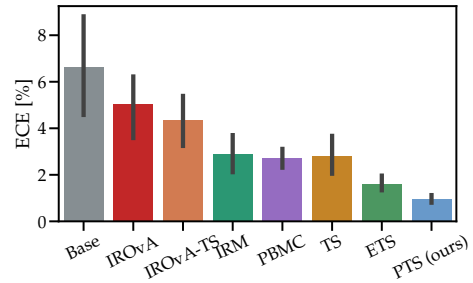


Figure 2: Bars show the average ECE of all baseline methods. Average is taken over all architectures and baselines and lines indicate standard deviation. PTS improves substantially over all baselines with relative reduction of calibration error of 39% over ETS and even higher reductions for other baselines.

\hat{Y} via the softmax function σ_{SM} as $\hat{P} = \max_c \sigma_{SM}(\hat{Z})^{(c)}$. In this work, we develop a new approach to improve the quality of the predictive uncertainty of h by improving the calibration of its confidence scores \hat{P} .

Uncertainty (miss-)calibration We define perfect calibration such that accuracy and confidence match for all confidence levels [5]:

$$\mathbb{P}(\hat{Y} = Y | \hat{P} = p) = p, \quad \forall p \in [0, 1] \quad (2)$$

Based on equation 2 it is straight-forward to define miss-calibration as the difference in expectation between confidence and accuracy:

$$\mathbb{E}_{\hat{P}} [|\mathbb{P}(\hat{Y} = Y | \hat{P} = p) - p|] \quad (3)$$

Measuring calibration The expected calibration error (ECE) [14] is a scalar summary measure estimating

Table 2: Expected calibration error ECE_{hist} . Results are largely consistent with ECE¹: our approach (PTS) outperforms all other approaches in most settings.

	Base	IROvA	IROvA-TS	IRM	PBMC	TS	ETS	PTS
CIFAR_LeNet5	2.02	2.05	1.9	1.11	2.37	1.78	1.61	1.38
CIFAR_VGG19	7.92	1.14	0.76	0.9	1.33	1.66	1.42	0.64
CIFAR100_LeNet5	7.55	1.8	2.5	3.46	2.54	1.96	1.06	1.08
CIFAR100_VGG19	12.96	5.68	2.77	5.36	3.02	3.7	2.4	1.06
Imagenet_ResNet50	6.17	6.6	5.65	2.87	3.42	1.77	1.32	0.84
Imagenet_ResNet152	6.27	6.41	5.49	2.96	3.42	2.19	1.44	0.91
Imagenet_VGG19	2.07	6.1	5.89	1.83	3.17	2.04	1.41	0.91
Imagenet_DenseNet169	6.12	6.64	5.63	2.83	3.37	1.94	1.3	0.89
Imagenet_EfficientNetB7	3.14	6.19	6.05	2.92	1.33	5.9	2.92	1.45
Imagenet_Xception	13.25	8.42	5.43	5.33	3.04	4.42	2.09	1.02
Imagenet_MobileNetV2	5.36	4.48	5.5	1.99	1.78	3.28	1.75	1.18

miss-calibration by approximating equation 3 based on predictions, confidence scores and ground truth labels $\{(Y_l, \hat{Y}_l, \hat{P}_l)\}_{l=1}^L$ of a finite number of L samples. ECE is computed by first partitioning all L confidence scores \hat{P}_l into M equally sized bins of size $1/M$ and computing accuracy and average confidence of each bin. Let B_m be the set of indices of samples whose confidence falls into its associated interval $I_m = (\frac{m-1}{M}, \frac{m}{M}]$. $\text{conf}(B_m) = 1/|B_m| \sum_{i \in B_m} \hat{P}_i$ and $\text{acc}(B_m) = 1/|B_m| \sum_{i \in B_m} \mathbf{1}(\hat{Y}_i = Y_i)$ are the average confidence and accuracy associated with B_m , respectively. The ECE is then computed as

$$ECE^d = \sum_{m=1}^M \frac{|B_m|}{n} \|\text{acc}(B_m) - \text{conf}(B_m)\|_d \quad (4)$$

with d usually set to 1 for the 11-norm. While the ECE is the most commonly used measure of miss-calibration, it has some drawbacks. In particular, the choice of bins can result in biased estimates and/or volatility [1, 10, 24]. Therefore, alternative formulations to mitigate these issues have been suggested. For example, [24] have proposed to replace histograms with non-parametric density estimators and present an ECE based on kernel density estimation (KDE).

4 Highly expressive post-hoc calibration via parameterized temperature scaling

To overcome limitations in the expressive power of TS-based methods, we propose to parameterize the temperature in a flexible and expressive manner. Rather than learning a single temperature (or weighted sum of fixed temperatures), we introduce a dependency of the temperature on the un-normalized logits. In other words, while temperature scaling works by re-scaling

any logit tuple of a trained model by the same temperature, PTS introduces a dependency of the temperature on the logit tuple itself. That is, our approach leverages the information present in a logit tuple to compute a prediction-specific temperature.

More formally, we propose the following post-hoc calibrator to map unnormalized logits \mathbf{z} to calibrated confidence scores. We start by parameterizing the temperature T with a flexible neural network as follows:

$$T(\mathbf{z}; \boldsymbol{\theta}) = g_{\boldsymbol{\theta}}(\mathbf{z}^s) \quad (5)$$

with $\boldsymbol{\theta}$ being the weights of a neural network g parameterizing the scalar temperature $T(\mathbf{z}; \boldsymbol{\theta})$ and \mathbf{z}^s being an unnormalized logit tuple sorted by decreasing value. The parameterized temperature is then used to obtain calibrated confidence scores \hat{Q}_i for sample i based on unnormalized logits \mathbf{z}_i :

$$\hat{Q}_i(\mathbf{z}_i, \boldsymbol{\theta}) = \max_c \sigma_{SM}(\mathbf{z}_i / T(\mathbf{z}_i; \boldsymbol{\theta}))^{(c)} \quad (6)$$

$$= \max_c \sigma_{SM}(\mathbf{z}_i / g_{\boldsymbol{\theta}}(\mathbf{z}_i^s))^{(c)} \quad (7)$$

We fit a post-hoc calibrator for a trained neural network $h(X)$ by optimizing an ECE²-based loss with respect to $\boldsymbol{\theta}$:

$$L_{ECE} = \sum_{m=1}^M \frac{|B_m|}{n} \left\| \text{acc}(B_m) - \frac{1}{|B_m|} \sum_{i \in B_m} \hat{Q}_i(\mathbf{z}_i, \boldsymbol{\theta}) \right\|_2 \quad (8)$$

with \mathbf{z}_i being the output of $h(X_i)$ in form of an unnormalized logit tuple and $\hat{Q}_i(\mathbf{z}_i, \boldsymbol{\theta})$ its confidence score transformed with the parameterized temperature $T(\mathbf{z}_i; \boldsymbol{\theta})$ (as defined in eq. 7). B_m and $\text{acc}(B_m)$ are

Table 3: Expected calibration error ECE_{KDE}. Overall rankings are largely consistent with ECE¹.

	Base	IROvA	IROvA-TS	IRM	PBMC	TS	ETS	PTS (ours)
CIFAR_LeNet5	1.94	1.8	1.83	1.22	2.34	1.98	1.82	1.6
CIFAR_VGG19	7.35	1.26	1.11	1.07	1.93	1.85	1.73	1.24
CIFAR100_LeNet5	7.55	1.76	2.67	3.35	2.7	1.73	1.07	1.24
CIFAR100_VGG19	12.32	5.29	2.5	5.14	3.74	3.44	2.32	1.14
Imagenet_ResNet50	5.62	5.94	5.0	2.55	4.83	1.44	1.57	1.18
Imagenet_ResNet152	5.69	5.73	4.83	2.48	4.88	1.85	1.4	1.24
Imagenet_VGG19	1.46	5.49	5.28	1.38	4.5	1.77	1.3	0.98
Imagenet_DenseNet169	5.49	5.95	4.97	2.4	4.81	1.53	1.29	1.24
Imagenet_EfficientNetB7	3.11	5.76	5.64	2.94	2.09	5.92	3.02	1.55
Imagenet_Xception	12.6	7.72	4.79	4.77	3.62	4.01	1.98	1.15
Imagenet_MobileNetV2	5.66	4.04	5.0	1.87	3.17	3.14	1.99	1.59

computed as described above, based on L ground truth labels, predictions and transformed confidence scores $\{(Y_l, \hat{Y}_l, \hat{Q}_l\}_{l=1}^L$ of the validation set. PTS is summarized in Algorithm 1.

Like standard temperature scaling, PTS with a parameterized temperature $T(z^r; \theta)$ does not change the accuracy of the trained model since the ranking of the logits remains unchanged.

5 Experiments and results

We first explore the relation between calibration performance and expressive power of a post-hoc calibrator and demonstrate that performance of current state-of-the-art temperature-scaling based calibrators is limited by expressive power.

Next, we show that PTS is a one-size-fits-all approach for post-hoc calibration: in contrast to the common state-of the-art where performance varies widely between datasets and network architectures, our approach consistently outperforms state-of-the-art methods on a wide range of datasets and model architectures. We then demonstrate that in spite of the larger number of parameters, PTS has a similar data efficacy compared to low-parametric baselines such as temperature-scaling. Finally, in extensive ablation studies, we show that the better performance of PTS stems from PTS leveraging its expressive power from via an ECE-based loss function.

5.1 Baseline methods and datasets

We compare our approach to the following baseline methods:

- Base: Uncalibrated baseline model

- Temperature scaling (TS): Post-hoc calibration by temperature scaling [5]
- Ensemble Temperature scaling (ETS): Ensemble version of TS with 4 parameters [24]
- Isotonic regression (IR) [23]
- Accuracy preserving version of Isotonic regression (IRM) [24]
- Composite model combining Temperature Scaling and Isotonic Regression (TS-IR) [24]
- The scaling-binning calibrator, combining temperature scaling with histogram binning (PBMC) [10]

We evaluate the performance of all models on three datasets, namely Imagenet, CIFAR-10 and CIFAR-100. For all datasets, we we calibrate various neural network architectures. For CIFAR-10 and CIFAR-100, we train VGG19 [18] and LeNet5 [12]. For Imagenet we used 7 pre-trained models provided as part of tensorflow, namely ResNet50, ResNet152 [6], VGG19, DenseNet169 [8], EfficientNetB7 [19], Xception [3] and MobileNetv2 [17].

We used a standard setup for evaluating model calibration [5] and trained PTS as well as all baselines on the standard validation sets of all datasets. We then evaluated all models by computing the ECE on the standard test sets. For CIFAR-10 and CIFAR-100, we used a validation dataset consisting of 5000 samples and an independent test set of 10000 samples. For ImageNet, we randomly split the hold-out set into a validation set of 12500 samples and a test set of 37500 samples.

Algorithm 1 Parameterized Temperature Scaling (PTS)

Input: Trained classification model $(\hat{Y}, \hat{Z}) = h(X)$, validation set (X, Y) , initialized calibration network $T = g_\theta(Z)$, number of training steps S , batch size β .

- 1: **for** ζ in $1:S$ **do**
- 2: Read minibatch $MB = (\{X_1, \dots, X_\beta\}, \{Y_1, \dots, Y_\beta\})$ from validation set
- 3: **for** X_b in MB **do**
- 4: Compute calibrated predictions $\hat{Q}_b = \max_c \sigma_{SM}(\mathbf{z}_b / g_\theta(\mathbf{z}_b))^{(c)}$ with $\mathbf{z}_b = h(X_b)$ (eq. 7)
- 5: **end for**
- 6: Partition all Q_b into M equally spaced bins with $m_b \in \{1, \dots, M\}$ being the bin into which sample b falls.
- 7: Compute binned accuracy $\text{acc}(B_{m_b})$ for all samples b in MB , with B_{m_b} being the set of indices of samples falling in bin m_b
- 8: Compute L_{ECE} based on MB using eq. 4 and do one training step optimizing θ based on MB
- 9: **end for**

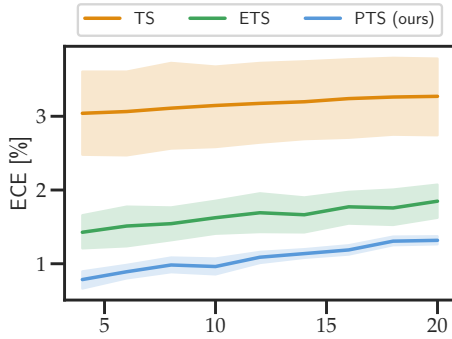


Figure 3: Mean ECE across 7 architectures trained on ImageNet, with a confidence band illustrating one standard deviation. PTS has the lowest calibration error across all architectures, irrespective of the chosen number of bins.

We quantify the quality of calibration for all experiments using the standard Expected Calibration Error ECE^1 based on 10 bins as well as and Expected Calibration Error based on kernel density estimates, ECE_{KDE} . In addition, we also report results from an alternative histogram-based formulation of ECE where bins are chosen such that each bin contains the same number of samples.

PTS was trained as a neural network with 2 fully connected hidden layers with 5 each. Hyperparameters were the same for all experiments, namely a learning rate of 0.0001, batch size of 1000 and stepsize of 100,000. We further limited \mathbf{z}^s to the top 10 most confident predictions in all settings since we found that they convey sufficient information.

5.2 Higher expressive power leads to better calibration performance

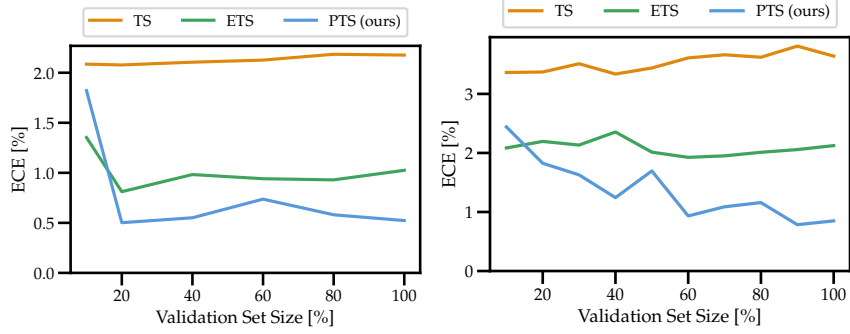
To assess the link between expressive power and calibration for temperature-scaling based models, we train

our PTS calibrators with an increasing number of nodes in the hidden layers on the Imagenet validation set. We compare calibration performance of our neural-network-based parameterization of the temperature to post-hoc calibrators with fixed temperature on the Imagenet test set. Fig. 1 illustrates that increasing the expressive power of temperature scaling (based on a single parameter) via a weighted ensembles of 3 temperatures (4 parameters) results in an improved ECE (53% for ResNet152 trained on ImageNet), as previously demonstrated. When further increasing the expressive power of temperature-scaling based calibrators via a neural network, we find that the calibration error further decreases with a larger number of parameters until a plateau is reached (additional improvement in ECE of 49% for ResNet152 trained on ImageNet). This illustrates that the performance of temperature-scaling based methods is limited by their inherent expressive power.

5.3 PTS is a one-size-fits-all post-hoc calibrator

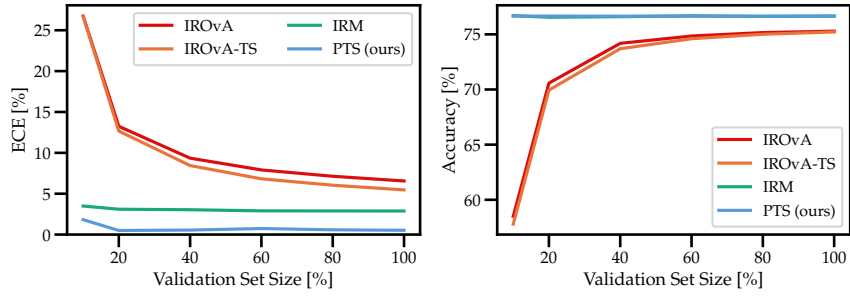
We next evaluate the performance of our approach on a total of 11 deep neural networks trained on CIFAR-10, CIFAR-100 and Imagenet.

Table 1 shows the standard ECE, Table 2 the KDE-based ECE and Table 3 ECE_{HIST} for all experiments. Rankings for both metrics are largely consistent and our approach outperforms baselines in all settings in terms of ECE^1 . ECE_{KDE} and ECE_{HIST} suggest that in settings with low complexity - i.e. a simple dataset with low number of classes such as CIFAR-10 and/or a simple architecture such as LeNet - performance of PTS is comparable to ETS only. The more complex a setting, the larger the gain of PTS. This range of complex architectures and datasets is particularly relevant in practice since [5] have shown that it is particularly modern architectures that are prone to mis-calibration. To make sure the choice of bin size when computing the ECE does not affect our findings, we computed ECE^1



(a) ECE for ResNet152 trained on ImageNet (b) ECE for VGG19 trained on CIFAR-100
for different validation set sizes for different validation set sizes

Figure 4: ECE for post-hoc calibrators trained on increasingly smaller subsets of the validation sets of ImageNet (a) and CIFAR-100 (b), generated by subsampling decreasing fractions of the full validation set (10% to 100%). PTS maintains the high data efficiency inherent in TS-based methods with low ECE even for small validation sets.



(a) ECE for ResNet152 trained on ImageNet (b) Accuracy for ResNet152 trained on ImageNet

Figure 5: ECE and accuracy for non-parametric post-hoc calibrators on validation sets of decreasing size. Non-parametric calibration methods suffer from a low data-efficiency and decrease in accuracy compared to PTS.

for bin sizes M ranging from 5 to 20 in steps of 2. Figure 3 illustrates the mean ECE across the 7 architectures trained on ImageNet and calibrated using TS, ETS and PTS. While small bin sizes result in a systematically smaller ECE - a known bias [10] - PTS outperforms the other TS-based methods for all bin sizes with rankings being unchanged.

5.4 PTS is data-efficient

A major advantage of TS-based models over other approaches is their high data-efficiency paired with accuracy-preserving properties. That is, even for small validation sets, this family of methods will yield improved calibration without affecting accuracy. We therefore designed experiments to quantify the data-efficiency of PTS. To this end, we fitted our model on increasingly smaller subsets of the validation set to calibrate a ResNet152 architecture trained on ImageNet and a VGG19 architecture trained on CIFAR-100. In both cases we varied the size of the subsets from

10% to 100% of the respective standard validation set size. When evaluating ECE on the test set, we found that like vanilla TS and ETS, our model yielded excellent performance even when trained on small fractions of the validation set, maintaining one of the key advantages of TS-based models (Figure 4).

These findings are in contrast to non-parametric models, which also tend to have a higher expressive power than standard TS approaches. When repeating the data-efficiency experiment for this family of models, we found that calibration error increased substantially with decreasing validation set size. In addition, IROVA and IROVA-TS also yielded a substantial decrease in accuracy (Figure 5).

5.5 Interplay between loss and expressive power

In contrast to modern TS-based models, which are optimized based on the mean squared error (mse) [24], PTS learns θ (parameterizing the temperature) by opti-

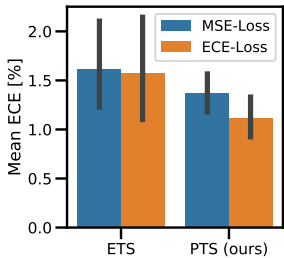


Figure 6: ETS and PTS models trained with different loss functions

mizing an ECE-based loss. To investigate the interplay between loss function and expressive power, we conduct a set of experiments where we combine different loss functions with TS-based models of different expressive power. More specifically, we fit ETS and PTS by optimizing mse and ECE for all 7 architectures trained on ImageNet.

Figure 6 illustrates that using the ECE loss during training only results in a significant benefit in terms of test ECE for our highly expressive PTS model. In contrast, ETS is not sensitive to the choice in loss function and do not benefit from the ECE loss. This suggests that it is the interaction between high expressive power and a complex loss function that results in the large performance gains of PTS.

6 Conclusion

In this work, we have introduced a novel approach for accuracy-preserving post-hoc calibration by modeling prediction-specific temperatures. To boost the expressive power of TS-based models we introduce a dependency of the temperature on the predicted logits and propose a parameterization of the temperature itself using a neural network. These prediction-specific temperatures make up a highly expressive, accuracy-preserving and data-efficient generalization of temperature scaling. In extensive experiments, we show that this approach results in substantially lower calibration errors than existing post-hoc calibration approaches, with an average improvement over the current state-of-the-art (ETS) of 39%.

References

- [1] A. Ashukha, A. Lyzhov, D. Molchanov, D. Vetrov, Pitfalls of in-domain uncertainty estimation and ensembling in deep learning, arXiv preprint arXiv:2002.06470.
- [2] C. Blundell, J. Cornebise, K. Kavukcuoglu, D. Wierstra, Weight uncertainty in neural networks, arXiv preprint arXiv:1505.05424.
- [3] F. Chollet, Xception: Deep learning with depthwise separable convolutions, in: Proceedings of the IEEE conference on computer vision and pattern recognition, 2017, pp. 1251–1258.
- [4] A. Graves, Practical variational inference for neural networks, in: Advances in neural information processing systems, 2011, pp. 2348–2356.
- [5] C. Guo, G. Pleiss, Y. Sun, K. Q. Weinberger, On calibration of modern neural networks, in: Proceedings of the 34th International Conference on Machine Learning-Volume 70, JMLR. org, 2017, pp. 1321–1330.
- [6] K. He, X. Zhang, S. Ren, J. Sun, Deep residual learning for image recognition, in: Proceedings of the IEEE conference on computer vision and pattern recognition, 2016, pp. 770–778.
- [7] G. Hinton, D. Van Camp, Keeping neural networks simple by minimizing the description length of the weights, in: in Proc. of the 6th Ann. ACM Conf. on Computational Learning Theory, Citeseer, 1993.
- [8] G. Huang, Z. Liu, L. Van Der Maaten, K. Q. Weinberger, Densely connected convolutional networks, in: Proceedings of the IEEE conference on computer vision and pattern recognition, 2017, pp. 4700–4708.
- [9] D. P. Kingma, T. Salimans, M. Welling, Variational dropout and the local reparameterization trick, in: Advances in Neural Information Processing Systems, 2015, pp. 2575–2583.
- [10] A. Kumar, P. S. Liang, T. Ma, Verified uncertainty calibration, in: Advances in Neural Information Processing Systems, 2019, pp. 3792–3803.
- [11] B. Lakshminarayanan, A. Pritzel, C. Blundell, Simple and scalable predictive uncertainty estimation using deep ensembles, in: Advances in Neural Information Processing Systems, 2017, pp. 6402–6413.
- [12] Y. LeCun, L. Bottou, Y. Bengio, P. Haffner, Gradient-based learning applied to document recognition, Proceedings of the IEEE 86 (11) (1998) 2278–2324.
- [13] D. Milios, R. Camoriano, P. Michiardi, L. Rosasco, M. Filippone, Dirichlet-based gaussian processes for large-scale calibrated classification, arXiv preprint arXiv:1805.10915.

- [14] M. P. Naeini, G. Cooper, M. Hauskrecht, Obtaining well calibrated probabilities using bayesian binning, in: Twenty-Ninth AAAI Conference on Artificial Intelligence, 2015.
- [15] R. M. Neal, Bayesian learning for neural networks, Vol. 118, Springer Science & Business Media, 2012.
- [16] J. C. Platt, Probabilistic outputs for support vector machines and comparisons to regularized likelihood methods, in: ADVANCES IN LARGE MARGIN CLASSIFIERS, MIT Press, 1999, pp. 61–74.
- [17] M. Sandler, A. Howard, M. Zhu, A. Zhmoginov, L.-C. Chen, Mobilenetv2: Inverted residuals and linear bottlenecks, in: Proceedings of the IEEE conference on computer vision and pattern recognition, 2018, pp. 4510–4520.
- [18] K. Simonyan, A. Zisserman, Very deep convolutional networks for large-scale image recognition, arXiv preprint arXiv:1409.1556.
- [19] M. Tan, Q. V. Le, Efficientnet: Rethinking model scaling for convolutional neural networks, arXiv preprint arXiv:1905.11946.
- [20] M. Welling, Y. W. Teh, Bayesian learning via stochastic gradient langevin dynamics, in: Proceedings of the 28th international conference on machine learning (ICML-11), 2011, pp. 681–688.
- [21] J. Wenger, H. Kjellström, R. Triebel, Non-parametric calibration for classification, in: International Conference on Artificial Intelligence and Statistics, PMLR, 2020, pp. 178–190.
- [22] B. Zadrozny, C. Elkan, Obtaining calibrated probability estimates from decision trees and naive bayesian classifiers, in: Icml, Vol. 1, Citeseer, 2001, pp. 609–616.
- [23] B. Zadrozny, C. Elkan, Transforming classifier scores into accurate multiclass probability estimates, in: Proceedings of the eighth ACM SIGKDD international conference on Knowledge discovery and data mining, 2002, pp. 694–699.
- [24] J. Zhang, B. Kailkhura, T. Han, Mix-n-match: Ensemble and compositional methods for uncertainty calibration in deep learning, arXiv preprint arXiv:2003.07329.